The Pennsylvania State University

The Graduate School

Department of Electrical Engineering

INVESTIGATION OF OPTICAL STRUCTURES FOR

ENHANCING THE LIGHT EXTRACTION EFFICIENCY OF WHITE LED

A Thesis in

Electrical Engineering

by

Wei-Liang Chen

Submitted in Partial Fulfillment
of the Requirements
for the Degree of

Master of Science

December 2009

The thesis of Wei-Liang Chen was reviewed and approved* by the following:

Shizhuo Yin
Professor of Electrical Engineering
Thesis Advisor

James K. Breakall
Professor of Electrical Engineering

Ken Jenkins
Professor of Electrical Engineering
Head of the Department

*Signatures are on file in the Graduate School

ABSTRACT

Recently, phosphor-conversion has been widely used in producing white light-emitting diodes (LEDs). In phosphor-converted (pc) LEDs, the blue LED chip is surrounded by the phosphor medium. When the blue light strikes the phosphor, some of the blue light is converted to yellow light, and the combination of two complementary lights produce the white light. In this method, the internal quantum efficiency could reach almost 100%; however, the light extraction efficiency of LED is still low.

In this thesis, we add a Bragg reflector to the LED between the blue light chip and the yellow light phosphor layer. The reflector can reflect the backward yellow light and allow the forward blue light, and enhancement of the light extraction efficiency of LED is achieved. All of the optical models and simulations are made by ray-tracing software ZEMAX.

TABLE OF CONTENTS

LIST OF FIGURES

LIST OF TABLES

Chapter 1

Introduction

1.1 Overview

The light-emitting diode (LED) is considered the next generation lighting source. In the United States, the Department of Energy (DOE) defined the goal of the solid state lighting (SSL) portfolio to reproduce 50 percent system efficiency:

> "By 2025, develop advanced solid state lighting technologies that, compared to conventional lighting technologies, are much more energy efficient, longer lasting, and cost-competitive by targeting a product system efficiency of 50 percent with lighting that accurately reproduces sunlight spectrum."

The Optoelectronics Industry Development Association's (OIDA) goal is to achieve 200 lm / W efficiency with high color rendering index by 2020.

In Europe, as of January 1st 2009, 75 watt, 100 watt and 150 watt incandescent bulbs are no longer sold in the United Kingdom (UK), and by 2010 the 40 watt incandescent bulbs will also disappear from store shelves. The European Union (EU) also agreed to an incandescent bulb phaseout starting in 2009 to be completed by 2012. After the phaseout is complete, the EU will save nearly 40 terrawatt hours of electricity per year. This is equivalent to the electricity usage of the entire country of Romania, and will eliminate about 15 million tons of CO_2 emission per year.

1.2 Advantages and weaknesses of LED

With the development of SSL technology, more and more applications of LEDs will be seen. Advantages and weaknesses of using LEDs are discussed below.

Advantages:

- Long lifespan

  The lifetime of conventional incandescent lamps is about 3000 ~ 4000 hours, while the estimated time to failure (ETTF) for the LED lamps can reach 100000 hours.

- Energy saving

  LEDs are more efficient than conventional lighting sources such as fluorescent and incandescent lamps. This is the most important reason for people to use LEDs as the next generation.

- More environmentally friendly

  LEDs contain no mercury unlike fluorescent bulbs and do not rely on a filament that may burn out, become heated, or disperse toxic gas.

- A variety of applications

  LEDs have advanced from use in indicators to many applications, including automotive lighting, displays, and illumination.

Weaknesses:

- Bad color revivication

  The color rendering index of LEDs is relatively low compared to incandescent bulbs. The color rendering index (CRI) of incandescent lamp is 100 while the white light LED has a CRI between 70 ~ 85. However, with the improvement of phosphor and the usage of new LED materials, some LEDs can reach a 90 CRI value.

- Single chip’s power is low

  Due to the low power of a single LED chip, its luminance remains fairly low. More LEDs are required in a device to reach the brightness needed, increasing the cost.

- Cost consideration

A 60 W incandescent bulb can generate about 1000 lm at an initial cost of about 1 dollar. Over the bulb lifespan, the operating cost is about 12 dollars, which is much more than the initial cost. In contrast, the operating cost for today's LEDs is about 3 dollars over the lifespan. However, the initial cost may be 30 dollars to buy a 1000 lm LED.

1.3 Fundamentals of LED

An LED can emit light under a forward bias. It has a p-n junction that many different materials may be used. Depending on the semiconductor material used, the wavelength or color of the emitted light can be different as shown in Table 1-1. Most commercially available LEDs are made from III-V compound semiconductors [1].

Table **1-1**: The color of LEDs which are manufactured from different semiconductor material [1].

Semiconductor Material	Color of LEDs
AlGaAs	red and infrared
AlGaP	Green
AlGaInP	high-brightness orange-red, orange, yellow, and green
GaAsP	red, orange-red, orange, and yellow
GaP	red, yellow, and green
GaN	green, pure green (or emerald green), and blue
InGaN	near ultraviolet, bluish-green and blue
SiC as substrate	blue
Si as substrate	blue
Sapphire (Al_2O_3) as substrate	blue
ZnSe	blue
C	ultraviolet
AlN, AlGaN	near to far ultraviolet

The first commercially usable LED was developed in 1962 using a compound semiconductor, GaAsP, which emitted a 655 nm red light [2]. Though the first LEDs had a relatively low efficiency, they still found use in a variety of applications, primarily as indicators.

In the early 1980s, the performance of red LED had increased to a practical level compared to conventional lighting sources [3]. In the 1990s, the development of the blue or green light LED made by GaN reached the efficiency of 30 lumens per watt. This provided the possibility of producing a white light source using LEDs by mixing different colors of light.

Current commercial white LEDs are available at 100 lumens per watt. They are expected to achieve a goal of 200 lumens per watt in the near future [4]. The applications of initial LEDs are mainly for indicators and numeric displays due to some limitations in color and efficiency. Over the past few years, the field of LED technology has been improving, and devices that have higher efficiencies and new colors have been fabricated in recent years. These improvements make LEDs useful for many applications, and will make the white light LEDs a viable replacement to traditional lighting sources over future years.

1.4 White LED

There are two methods used to produce white light with LEDs, phosphor conversion and the RGB system. Phosphor conversion uses a blue or ultraviolet (UV) chip surrounded by phosphors to emit white light. RGB system uses multiple monochromatic LEDs in red, green and blue and mixes them to produce the white light.

The most common used phosphor conversion method is using a blue LED to excite a yellow phosphor medium. When blue light strikes the phosphor layer, some portion of the blue light is converted to yellow light. With proper portion of mixture, the remaining blue light and the yellow light could produce the white light.

The three primary colors – red, green, and blue, can also be mixed to produce white light. Sometimes amber is added in order to enhance the color quality by filling in the yellow region of the spectrum.

1.5 Motivation

In order to replace conventional lighting sources, such as the fluorescent or incandescent lamp in the near future, high power white LEDs have attracted much interest as a possible solution [5].

In developing solid-state lighting based on LEDs, light extraction efficiency is an important issue. Nowadays epitaxy technology is mature and the internal quantum efficiency (IQE) could achieve 90%, possibly even up to 99% [6]. However the light extraction efficiency is relatively low. In this work we attempt to simulate the model of different structures and to study the change of light extraction efficiency.

Chapter 2

Basic Theory

The electrical and optical properties of the p-n junction and semiconductor materials need to be understood. This chapter describes the concepts of LEDs which involved with the interaction between semiconductor and light. Optical theories used in our research are also described.

2.1 Basic electroluminescence theory

As shown in Fig. 2-1, when p-type and n-type semiconductors are in contact with each other, the p-n junction forms a barrier for electrons between the p-type and n-type regions. Only by applying sufficient voltage to the semiconductor device, can the electrons can move from p-type area to the n-type area. The output light of the LEDs originates from the spontaneous emission in the p-n junction regions, which in turn is a radiation due to the recombination of the electrons and holes.

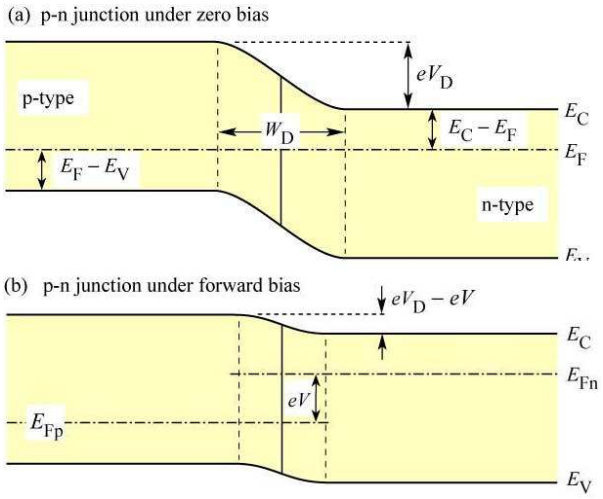

Figure **2-1**: LED p-n junction under (a) zero bias and (b) forward bias.[7]

2.2 Internal, extraction, and external efficiency

The internal, extraction and external efficiency for LEDs were well defined in [7]. Under an ideal situation, the active layer emits one photon for every electron-hole pair recombined. The Internal quantum efficiency (IQE) is defined as

$$\eta_{\text{int}} = \frac{\#\text{ of photons emitted form active region per second}}{\#\text{ of electrons injected into LED per second}} = \frac{P_{\text{int}}(h\nu)}{I/e}. \tag{2.1}$$

However, in the reality, a portion of the light emission is trapped in the in the LED, thus only a part of it emits into free space. There are two main reasons for this situation: absorption and total internal reflection (TIR). These phenomena reduce the probability of the light escaping from the LED chip. The light extraction efficiency (LEE) is defined as

$$\eta_{extraction} = \frac{\#\text{ of photons emitted into free space per second}}{\#\text{ of photons emitted from active region per second}} = \frac{P/h\nu}{P_{\text{int}}/h\nu}. \tag{2.2}$$

The external quantum efficiency (EQE) is defined as

$$\eta_{ext} = \frac{\#\text{ of photons emitted into free space per second}}{\#\text{ of electrons injected into LED per second}} = \frac{P/h\nu}{I/h\nu} = \eta_{\text{int}} \times \eta_{extraction}. \qquad (2.3)$$

2.3 Law of reflection and refraction

When light rays are incident to a boundary between two transparent mediums like plastic or glass and air, some portion of the light rays are reflected back into the incident medium and others are refracted at this boundary. Fig. 2-2 shows this interaction. θ_1 is the angle of incidence and θ_2 is the angle of reflection in a material with an index of refraction n_i ; θ_r is the angle of refraction in a material n_r .

$$\theta_1 = \theta_2 \qquad (2.4)$$

The angle of incidence equals the angle of reflection. This equation is the first part of the law of reflection. And the second part of the law of reflection maintains that the incident ray, perpendicular to the surface boundary, and the reflected ray all lie in a plane called the plane-of-incidence.

$$n_i \sin\theta_1 = n_r \sin\theta_r \qquad (2.5)$$

This equation is the law of refraction, also known as Snell's Law. When $n_i < n_r$, it follows from Snell's Law that $\sin\theta_1 > \sin\theta_r$, and since the same function is every where positive between 0^o and 90^o, then $\theta_1 > \theta_r$. Rather than going straight through, the ray entering a higher-index medium bends toward the normal. The reverse is also true; that is, on entering a lower-index medium, the ray, rather than going straight through will bend away from the normal.

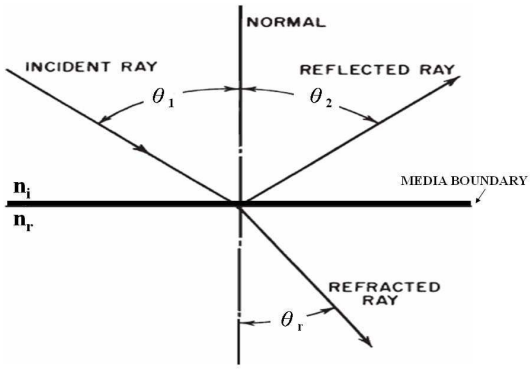

Figure **2-2**: Relationship between a ray incident on a plane surface and the reflected and refracted rays.

2.4 Total internal reflection (TIR)

When light propagates from a low refractive index medium to high refractive index medium, the angle of refracted light will be greater than the angle of incidence. When the angle of incidence equals the critical angle, the angle of refracted light will approach 90° and for a greater angle of incidence, the light will encounter total internal reflection. The critical angle can be obtained by Snell's law.

2.5 Transfer-matrix method for DBR

A distributed Bragg reflector (DBR) is a multilayer medium with a periodic structure having two different refractive index n_1 and n_2 and thicknesses a and b, which is shown in Fig. 2-3. Reference [8] has very detailed description of this method.

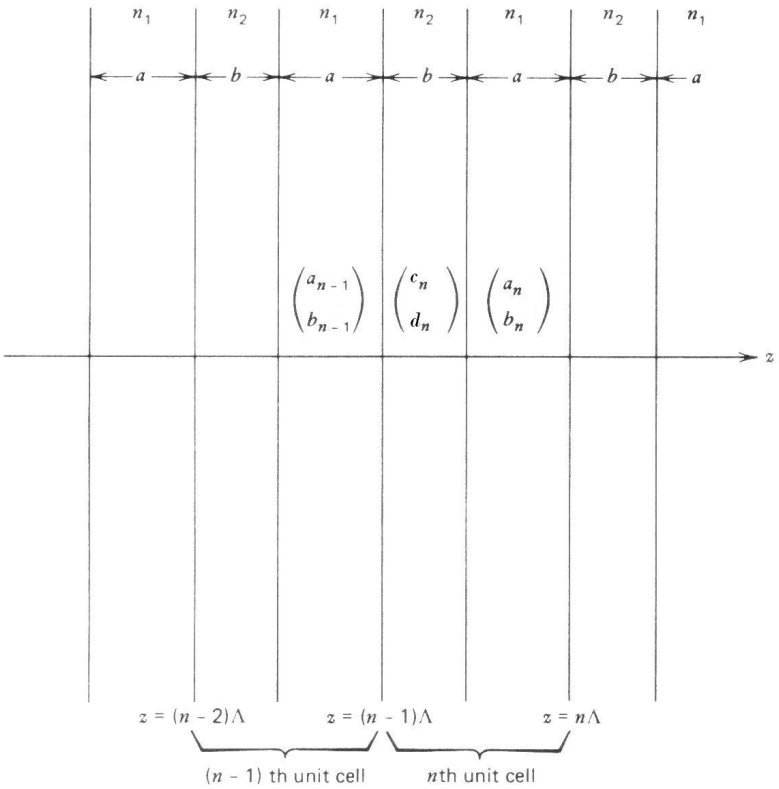

Figure **2-3**: DBR diagram [8]

We assume that both materials are isotropic. The periodic layered medium consists of two different materials with a refractive profile given by

$$n(z) = \begin{cases} n_2, 0 < z < b \\ n_{1,}, b < z < \Lambda \end{cases} \tag{2.6}$$

with

$$n(z) = n(z+\Lambda) \tag{2.7}$$

where b is the layer thickness with refractive index n_2, $a = \Lambda - b$ is the layer thickness with refractive index n_1. The z axis is normal to the layer interfaces, and $\Lambda = a+b$ is the period. We consider the light propagates in the yz plane. Since the medium is homogeneous in the y direction, a general wave equation can be written

$$E(y,z,t) = E(z)e^{i(\omega t - k_y y)} \tag{2.8}$$

where k_y is the y component of the wavevector of propagation, which remains constant throughout the medium. The electric field within each homogeneous layer can be expressed as a sum of a right-traveling (+z) and a left-traveling (-z) plane wave:

$$\begin{cases} a_n e^{-ik_{1z}(z-n\Lambda)} + b_n e^{+ik_{1z}(z-n\Lambda)}, n\Lambda - a < z < n\Lambda \\ c_n e^{-ik_{2z}(z-n\Lambda+a)} + d_n e^{+ik_{2z}(z-n\Lambda+a)}, (n-1)\Lambda < z < n\Lambda - a \end{cases} \tag{2.9}$$

with

$$k_{1z} = \sqrt{\left(\frac{n_1\omega}{c}\right)^2 - k_y^2}$$

$$k_{2z} = \sqrt{\left(\frac{n_2\omega}{c}\right)^2 - k_y^2}\,. \tag{2.10}$$

In the case of TE waves, imposing the continuity of E_x and H_y at the interfaces $z = (n-1)\Lambda$ and $z = n\Lambda - a$, we can obtain

$$a_{n-1} + b_{n-1} = c_n e^{ik_{2z}b} + d_n e^{-ik_{2z}b}$$

$$ik_{1z}(a_{n-1} - b_{n-1}) = ik_{2z}(c_n e^{ik_{2z}b} - d_n e^{-ik_{2z}b})$$

$$c_n + d_n = a_n e^{ik_{1z}a} + b_n e^{-ik_{1z}a}$$

$$ik_{2z}(c_n - d_n) = ik_{1z}(a_n e^{ik_{1z}a} - b_n e^{-ik_{1z}a})\,. \tag{2.11}$$

These equations could be written as two matrix equations:

$$\begin{bmatrix} 1 & 1 \\ ik_{1z} & -ik_{1z} \end{bmatrix}\begin{bmatrix} a_{n-1} \\ b_{n-1} \end{bmatrix} = \begin{bmatrix} e^{ik_{2z}b} & e^{-ik_{2z}b} \\ ik_{2z}e^{ik_{2z}b} & -ik_{2z}e^{-ik_{2z}b} \end{bmatrix}\begin{bmatrix} c_n \\ d_n \end{bmatrix}$$

$$\begin{bmatrix} 1 & 1 \\ ik_{2z} & -ik_{2z} \end{bmatrix}\begin{bmatrix} c_n \\ d_n \end{bmatrix} = \begin{bmatrix} e^{ik_{1z}a} & e^{-ik_{az}a} \\ ik_{1z}e^{ik_{1z}a} & -ik_{1z}e^{-ik_{1z}a} \end{bmatrix}\begin{bmatrix} a_n \\ b_n \end{bmatrix}. \tag{2.12}$$

By eliminating the column vector

$$\begin{bmatrix} c_n \\ d_n \end{bmatrix} \tag{2.13}$$

the matrix equation

$$\begin{bmatrix} a_{n-1} \\ b_{n-1} \end{bmatrix} = \begin{bmatrix} A & B \\ C & D \end{bmatrix}\begin{bmatrix} a_n \\ b_n \end{bmatrix} \tag{2.14}$$

can be obtained where the matrix elements are

$$A = e^{ik_{1z}a}\left[\cos k_{2z}b + \frac{i}{2}\left(\frac{k_{2z}}{k_{1z}} + \frac{k_{1z}}{k_{2z}}\right)\sin k_{2z}b\right]$$

$$B = e^{-ik_{1z}a}\left[\frac{i}{2}\left(\frac{k_{2z}}{k_{1z}} - \frac{k_{1z}}{k_{2z}}\right)\sin k_{2z}b\right]$$

$$C = e^{ik_{1z}a}\left[-\frac{i}{2}\left(\frac{k_{2z}}{k_{1z}} - \frac{k_{1z}}{k_{2z}}\right)\sin k_{2z}b\right]$$

$$D = e^{-ik_{1z}a}\left[\cos k_{2z}b - \frac{i}{2}\left(\frac{k_{2z}}{k_{1z}} + \frac{k_{1z}}{k_{2z}}\right)\sin k_{2z}b\right]. \tag{2.15}$$

For TM waves the matrix elements are

$$A = e^{ik_{1z}a}\left[\cos k_{2z}b + \frac{i}{2}\left(\frac{n_2^2k_{1z}}{n_1^2k_{2z}} + \frac{n_1^2k_{2z}}{n_2^2k_{1z}}\right)\sin k_{2z}b\right]$$

$$B = e^{-ik_{1z}a}\left[\frac{i}{2}\left(\frac{n_2^2 k_{1z}}{n_1^2 k_{2z}} - \frac{n_1^2 k_{2z}}{n_2^2 k_{1z}}\right)\sin k_{2z}b\right]$$

$$C = e^{ik_{1z}a}\left[-\frac{i}{2}\left(\frac{n_2^2 k_{1z}}{n_1^2 k_{2z}} - \frac{n_1^2 k_{2z}}{n_2^2 k_{1z}}\right)\sin k_{2z}b\right]$$

$$D = e^{-ik_{1z}a}\left[\cos k_{2z}b - \frac{i}{2}\left(\frac{n_2^2 k_{1z}}{n_1^2 k_{2z}} + \frac{n_1^2 k_{2z}}{n_2^2 k_{1z}}\right)\sin k_{2z}b\right]. \tag{2.16}$$

For a periodic multilayer structure, from (2.14)

$$\begin{bmatrix} a_0 \\ b_0 \end{bmatrix} = \begin{bmatrix} A & B \\ C & D \end{bmatrix}^n \begin{bmatrix} a_n \\ b_n \end{bmatrix}. \tag{2.17}$$

For calculating the reflection and transmission coefficients, we have

$$\begin{bmatrix} 1 \\ r \end{bmatrix} = \begin{bmatrix} A1 & B1 \\ C1 & D1 \end{bmatrix} \begin{bmatrix} t \\ 0 \end{bmatrix}. \tag{2.18}$$

The reflectivity coefficient is given by

$$r = \left(\frac{C1}{A1}\right). \tag{2.19}$$

Reflectance R is given by

$$R = |r|^2 = \left|\frac{C1}{A1}\right|^2 \tag{2.20}$$

and the transmittance T is given by

$$\text{T} = 1\text{-R}. \tag{2.21}$$

Chapter 3

Related Works

The development of high efficiency white LEDs has drawn people's attention for recent years. White light can be obtained in LEDs by using several different methods mentioned in chapter 1. For white light LEDs, the one most used is the phosphor conversion method [9]. Nowadays, the commercial white light pc-LEDs have relatively low light output and luminous efficiency. In order to achieve the goal of replacing the incandescent and fluorescent lamps by pc-LEDs, improvements are needed in several aspects, including (1) internal quantum efficiency, (2) extraction efficiency, and (3) phosphor-conversion efficiency. The increased luminous efficiency achieved improved during the past several years is primarily due to the improvements of the internal quantum efficiency and extraction efficiency.

As previously reported, the phosphor-conversion efficiency is low because a portion of the light is backscattered from the phosphor layer and huge loss happens due to absorption and TIR in the LED. Narendran et al. quantified the amount of forward and backward scattered light [10]. They found that about 40% of the light emission is forward scattered, and the remaining 60% goes backward into the LED body. This agrees with the results form Yamada et al [11]. This result shows a considerable loss because the phosphor emission could emit in a random direction. Therefore, reducing the phosphor conversion loss will help increase the efficiency. Several schemes have been proposed to improve the phosphor-conversion efficiency.

3.1 Scattered photon extraction (SPE)

As the first white light pc-LED was produced, the phosphor was placed around the chip. Since the late 1990s, the remote phosphor concepts were proposed for pc-LED [12][13][14]. The phosphor was moved away from the chip, as shown in Fig. 3-1.

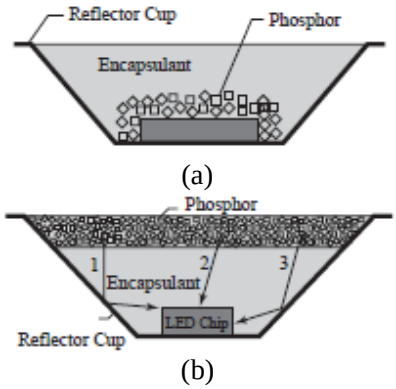

Figure **3-1**: (a) Conventional phosphor-in-cup LED that phosphor surrounds the chip (b) phosphor-on-top (remote phosphor) LED.[7]

In 2005, Narendran et al. [10] proposed a scattered photon extraction (SPE) pc-LED by moving the phosphor away from the chip and creating a custom optical element between the chip and the phosphor layer, as shown in Fig. 3-2. Their custom design of the optic transfers the blue light from chip to the phosphor medium and uses a transparent sidewall that allows most backward yellow emission from the phosphor layer to leave the LED.

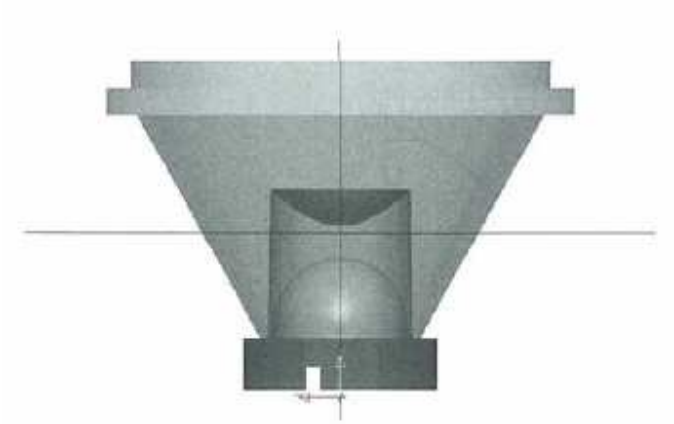

Figure **3-2**: White LED using SPE concept. [15]

3.2 The remote phosphor with hemispherical dome

Luo et al. [16] also proposed a packaging configuration that consists of a diffuse cup and a remote phosphor with hemispherical dome to reduce the light trapped between the phosphor layer and reflector cup, as shown in Fig. 3-3. The phosphor efficiency of it is 50% better than the phosphor-in-specular-cup with a flat encapsulation.

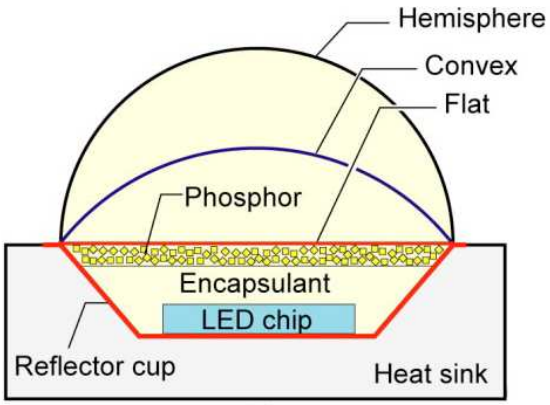

Figure **3-3**: Three different geometries of the encapsulation dome, flat (h=0), convex (h=r/2), and hemispherical (h=r) [16]

3.3 Effects of phosphor location on LED performance

In 2008, Liu et al. presented a comparison of the efficiency for five different packaging designs [17]. Based on the ray-tracing simulations, the result shows that remote phosphor design is more efficient and the designs with curved phosphor layer have higher light extraction efficiency than those of plane shape.

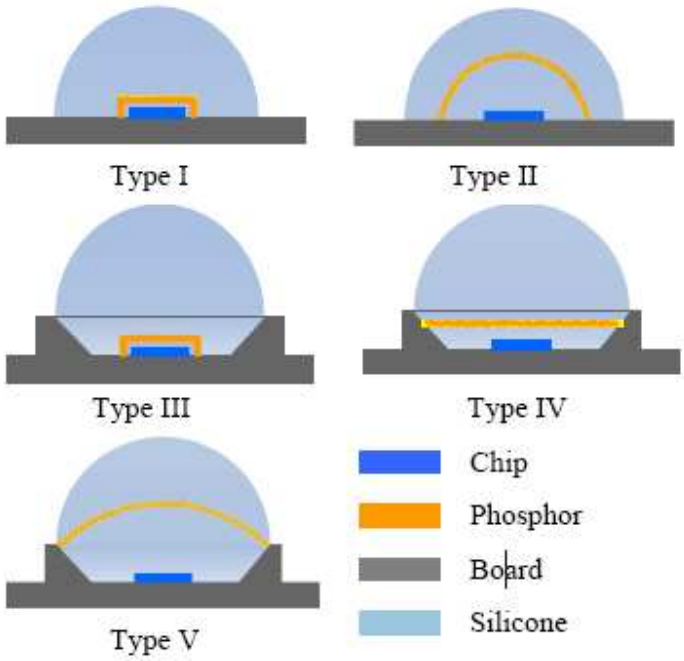

Figure **3-4**: Five types of packaging designs with different phosphor locations. [17]

3.4 Enhanced forward efficiency using short wave pass edge filter (SWPEF)

Earlier in 2009, Oh et al. proposed a scheme to recycle the backward emission of the yellow phosphor [18]. The LED structure is similar to a conventional remote pc-LED, but a dielectric multilayer, which allows blue light transmit it and reflect the yellow phosphor emission, was inserted between the LED chip and the phosphor layer.

Chapter 4

Experimental methods

In order to increase the phosphor conversion efficiency, this thesis proposes a method to reduce the light being trapped in the LED. We added a filter which allows yellow light to pass through but reflects blue light between the LED die and the phosphor layer. The filter can recycle the backward phosphor emission without blocking the blue light from striking the phosphor medium. Because a large portion of yellow phosphor emission goes backward, this design can increase the phosphor conversion efficiency.

4.1 Blue-pass yellow-reflection filter design

For a stack of periodic layers, omnidirectional reflection is the result of having a complete photonic bandgap. The light within the range of the bandgap, irrespective of polarization and incident angle, would be blocked by complete reflection. A conventional quarter-wave stack with two periodic refractive indices can be a candidate of a blue-pass yellow-reflection filter. However, the conventional quarter-wave stack shows obvious interferences in the transmission region as shown in Fig. 4-1(a). This ripple will increase the chance that blue light is blocked. To suppress the ripple a pair of eighth-wave low refractive index layers is added on both sides [19]. The numerical calculated reflection spectrum with suppressed ripple is shown in Fig. 4-1(b).

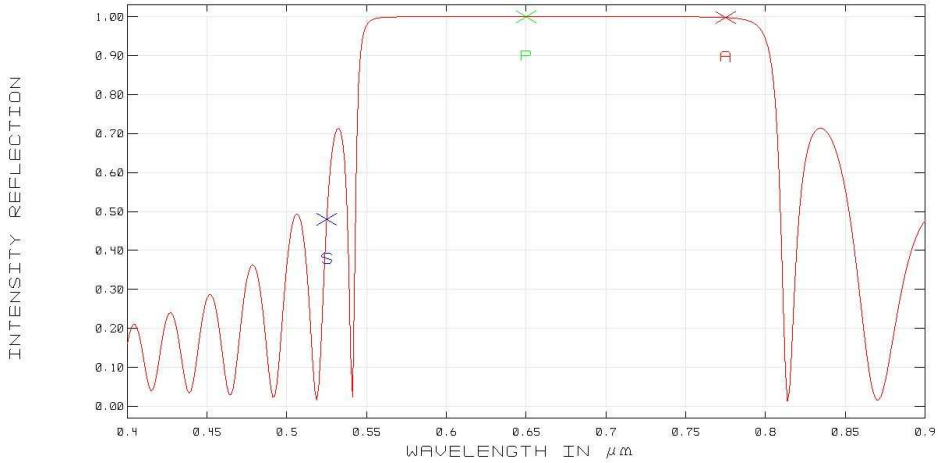

(a)

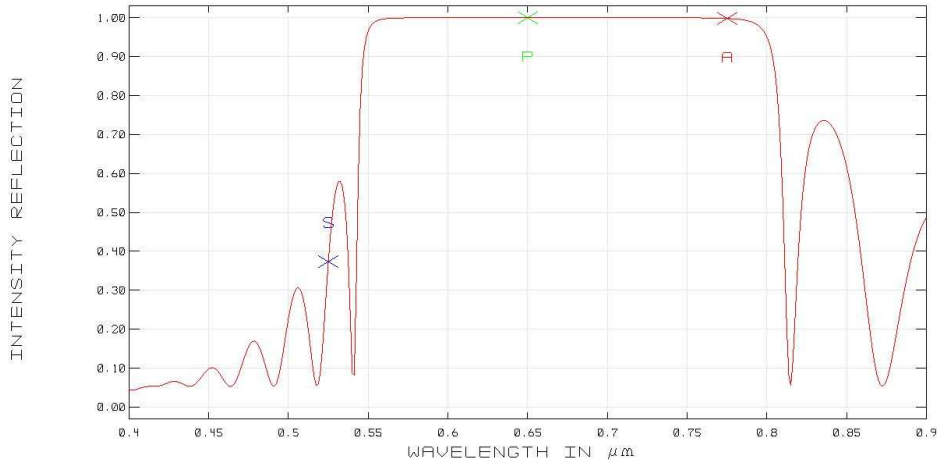

(b)

Figure **4-1**: (a) reflector without eighth wavelength layer shows obvious ripple (b) reflector with eighth wavelength layer shows ripple suppressed.

The tin (IV) sulfide-silica periodic structure is used to construct the filter. The refractive indices are n_1=2.6 and n_2=1.46 for tin sulfide (SnS_2) and silica (SiO_2), respectively. The filter made by tin sulfide and silica is reported having a golden appearance in white light and allows blue-green light to be transmitted through it [20]. The effect of the filter for different layer thicknesses, pairs of layers, and light incidence angles will be verified below.

A. Different layer thickness

A quarter-wave stack of SnS_2/SiO_2 reflector with 10 quarter-wave pairs is simulated first. The eighth-wave thick SiO_2 layer (55 nm) and quarter-wave thick SnS_2/SiO_2 (62 nm/110 nm) films performed a reflection band having a central wavelength at 650 nm with normal incidence. Changing the thickness of the thin film, different simulation results are shown in Fig. 4-2.

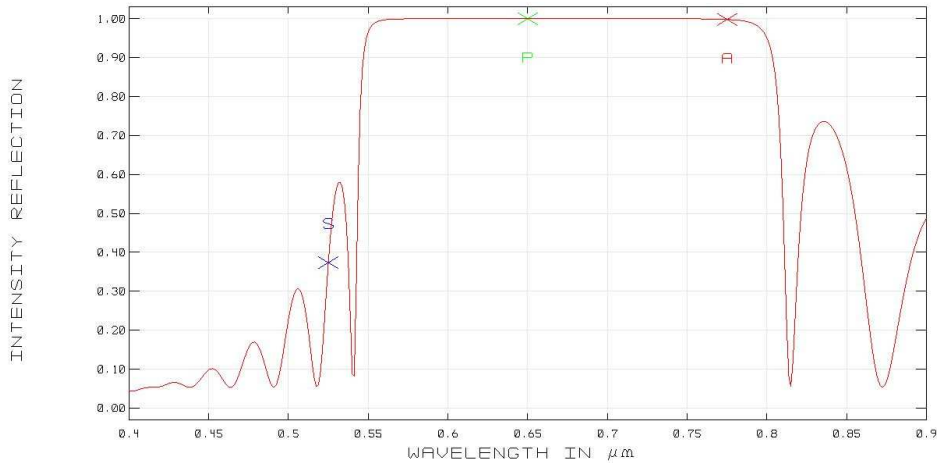

(a)

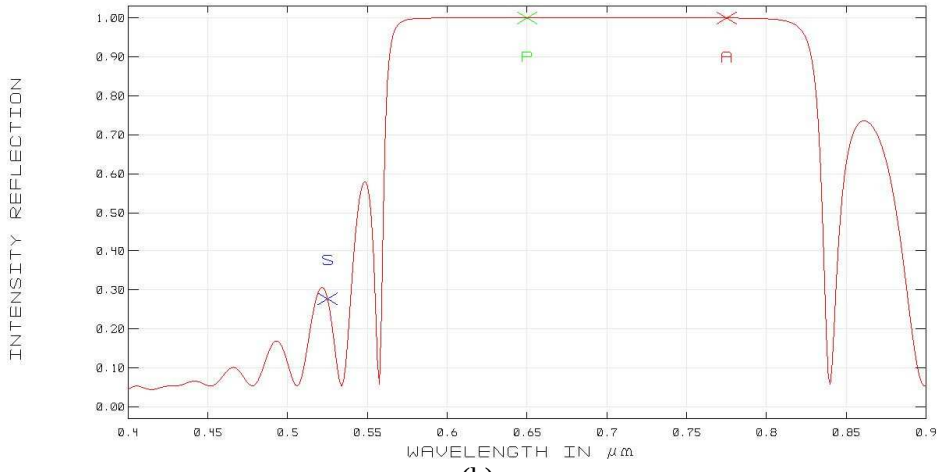

(b)

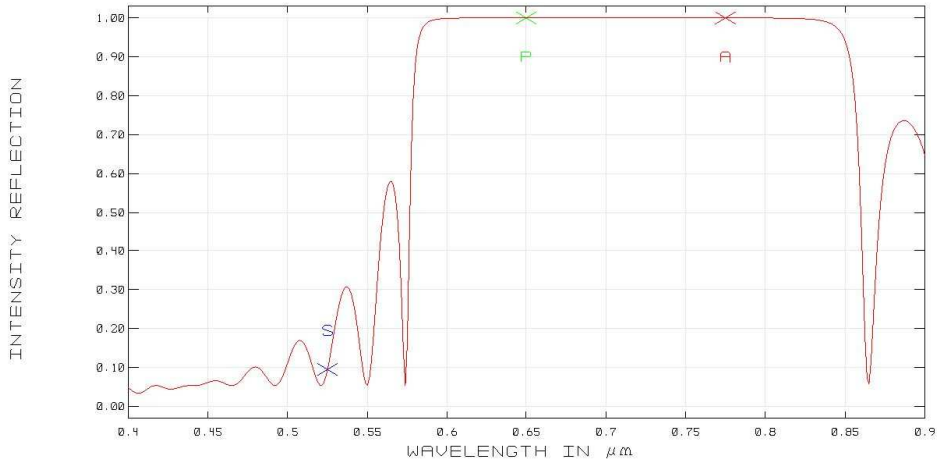

(c)

Figure **4-2**: Calculated reflectance spectra for normal incidence having central wavelength at (1) 650 nm (2) 670 nm (3) 690 nm

B. Different pairs of layers

The number of quarter-wave pairs in the stack was changed to view different effects. The results for different pairs are shown in Fig. 4-3. While the number of pairs goes up to 7, the reflectivity reaches 99% or higher for the reflection band.

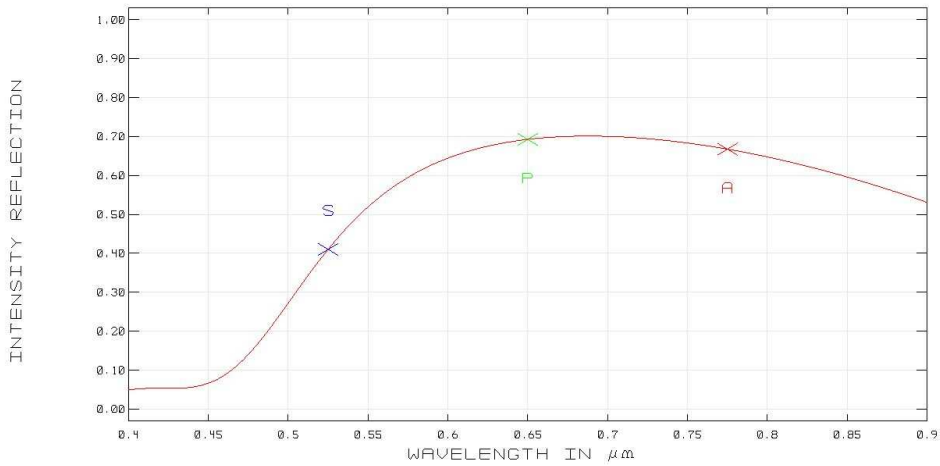

(a)

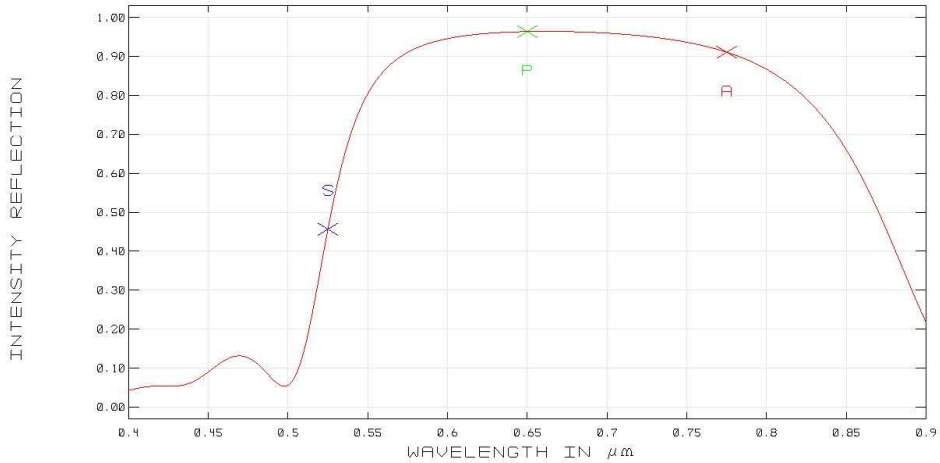

(b)

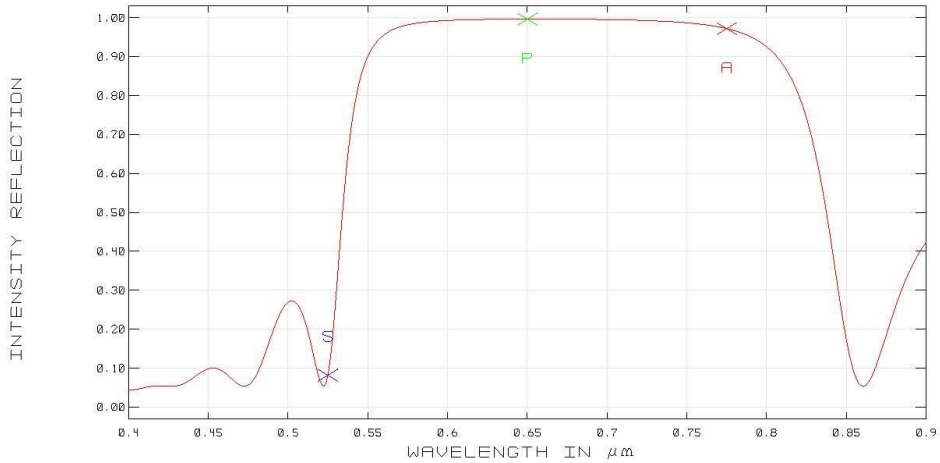

(c)

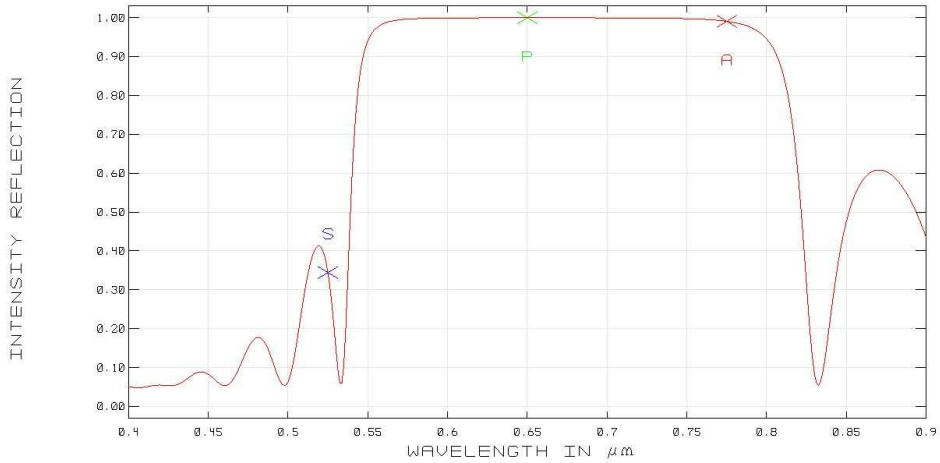

(d)

Figure **4-3**: Calculated reflectance spectra for normal incidence having (a)1 (b)3 (c)5 (d)7 pairs of periodic structure.

C. Different light incidence angle

Fig. 4-4 presents the numerically calculated reflectance spectrum of the quarter-wave SnS_2/SiO_2 reflector with a different incidence angle. Both angular and polarization influences of the reflection spectrum are illustrated. For TE waves, the reflection band expands as the incidence angle increases. On the contrary, for the TM waves, the reflection band shrinks as the incidence angle increases.

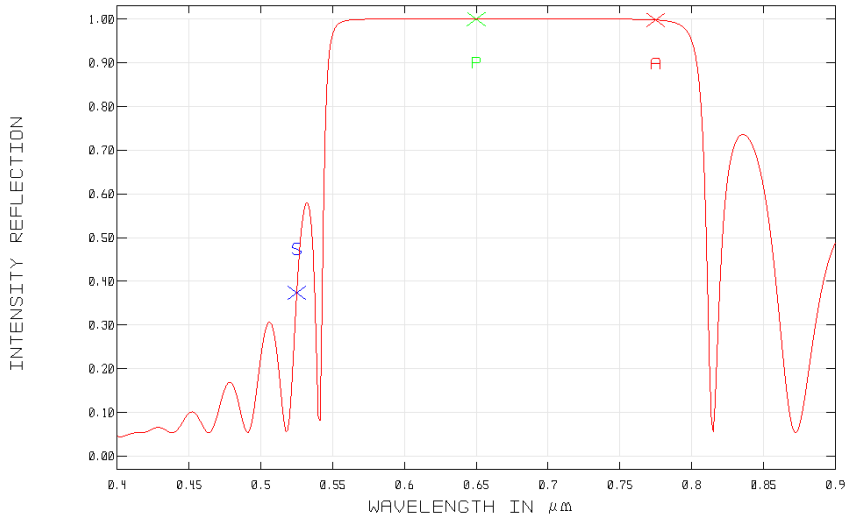

(a)

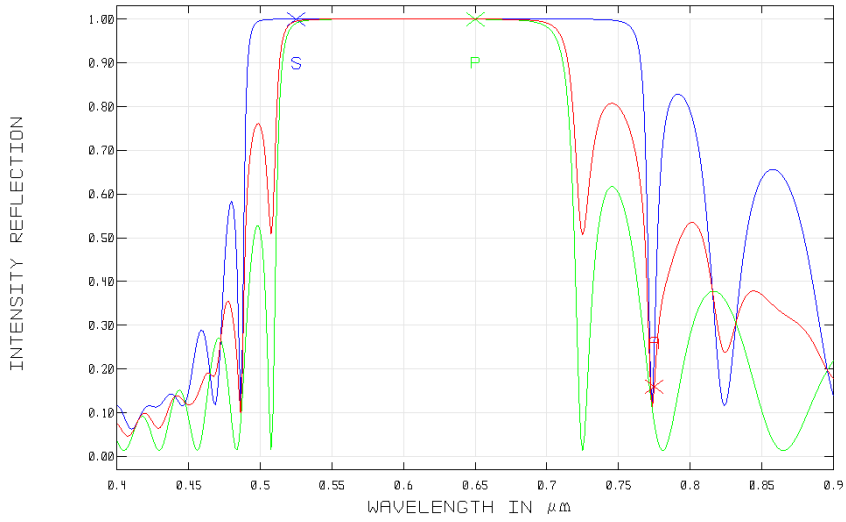

(b)

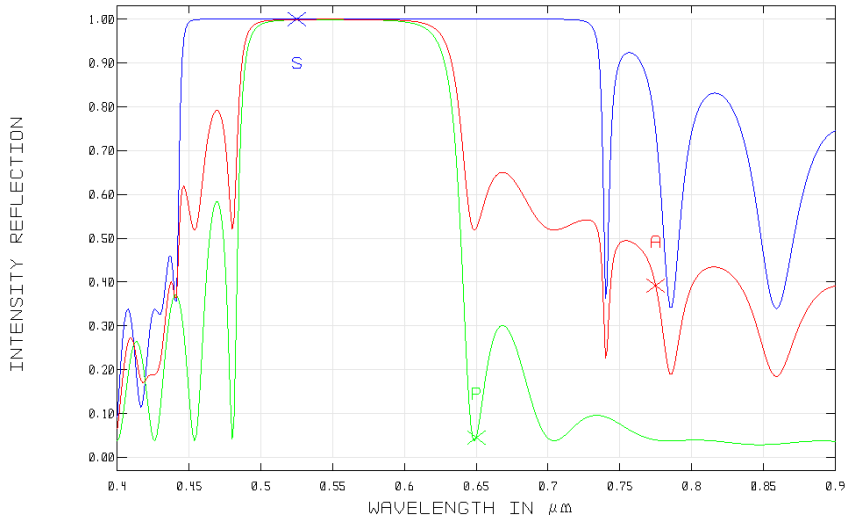

(c)

Figure **4-4**: Calculated reflectance spectra for (a) normal (b) 45 degree (c) 70 degree incidence. The green line is the result for TM wave; blue line for TE wave; and red line is the average.

4.2 Ray tracing analysis

A ray-tracing analysis was conducted by using ZEMAX. The LED configuration is shown in Fig. 4-5. The blue light LED chip is placed at the center of a hemispherical encapsulant. The dimensions of the chip are 1 mm by 1 mm and 0.3 mm height. The remote phosphor concept is used, where the phosphor is coated inside the encapsulant. The bottom surface of the structure has a 95% reflectance. A detector is placed 1 mm in front of the LED to measure the light intensity with different wavelengths. The optical ray-tracing analysis was conducted with the following assumptions:

A. The LED chip emits 440 nm light and the phosphor medium can convert a portion of 440 nm light into 560 nm light. The phosphor emission is omnidirectional, thus an equal amount of light goes forward and backward.

B. The encapsulant and the phosphor medium have refractive index 1.6 and both of them are transparent at the 440~560 nm. The phosphor layer is refractive matched to the encapsulant [22].

C. The mean-free-path (MFP) value is set to be 0.3 mm. The MFP denotes the average distance that the photon will travel before hitting with the phosphor article. One of the challenges in ray-tracing analysis is that the accurate MPF value is unknown. Zhu et al. introduced a method to determine the MFP. They made several experiments and ray-tracing simulations for different phosphor density, and the proper MFP values were obtained by matching the experimental results with ray-tracing simulations [15].

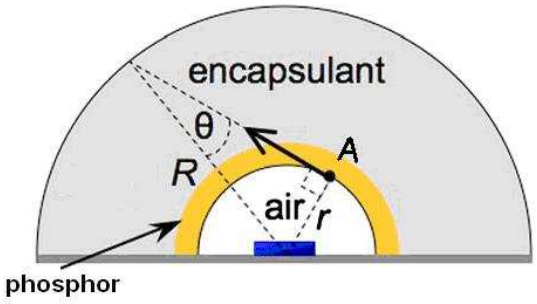

Figure **4-5**: The LED configuration of this thesis.[21]

Chapter 5

Results and discussion

Fig. 4-5 shows a schematic diagram used in the ray-tracing simulation. This white light LED combines two designs to increase the phosphor efficiency. First, the reflector is added between the inner air and phosphor interface to reduce the backward phosphor emission. Second, the hemisphere encapsulant design helps to avoid light being trapped in the encapsulant due to total internal reflection (TIR).

In order to reduce the amount of yellow light emitted backward into the chip, the phosphor should be placed far from the chip. However, to avoid the TIR of the phosphor emission at the exterior interface, the phosphor medium cannot be placed too close to the exterior interface.. Assuming the phosphor emission is from the point A in Fig. 4-5, the light will strike the exterior interface at the maximum angle θ. We can see that $\sin\theta = r/R$, where r is the radius of the inner air hemisphere and R is the radius of exterior encapsulant. To avoid TIR, $\sin\theta \leqq n_{air} / n_{encapsulant}$ or $r/R \leqq 1/n_{encapsulant}$ needs to be satisfied. Therefore, R should be longer than $n_{encapsulant} \times r$ to minimize the TIR. In our LED configuration, the $n_{encapsulant}$ is 1.6 and r/R is set to be 0.43 which qualifies the requirement to eliminate the TIR.

5.1 Increasing efficiency by adding reflector

The results from the optical ray-tracing are shown in Table 5-1.

Table **5-1**: The light intensity for different reflector applied.

	Yellow (W)	Blue (W)	Total (W)
No reflector applied	2.64	3.84	6.48
I (650 nm)	2.73	3.77	6.50
II (660 nm)	2.78	3.8	6.58
III (670 nm)	2.74	3.82	6.56
IV (680 nm)	2.71	3.8	6.51

We investigate several reflector designs which have central wavelengths of reflection bands at 650 nm, 660 nm, 670 nm, and 680 nm. They are made of the same materials but have different thickness for the layers. Our goal is to find the filter that allows most blue light transmitted and the most yellow light to be reflected . The optimal reflector should have a high reflectance in the yellow light region and high transmittance in the blue light region for any angle of incidence. We observed the reflectance spectrum for each design. The omnidirectional bandgap for each design is shown in Table 5-2. Fig. 5-1 is the calculated reflectance spectra at different incident angles (0º, 45º, and 70º) for TE and TM waves. The semitransparent yellow region shows the omnidirectional bandgap.

Table **5-2**: The omnidirectional bandgap of different reflectors.

	Omnidirectional bandgap
I (650 nm)	550 nm ~ 620 nm
II (660 nm)	560 nm ~ 630 nm
III (670 nm)	570 nm ~ 640 nm
IV (680 nm)	580 nm ~ 650 nm

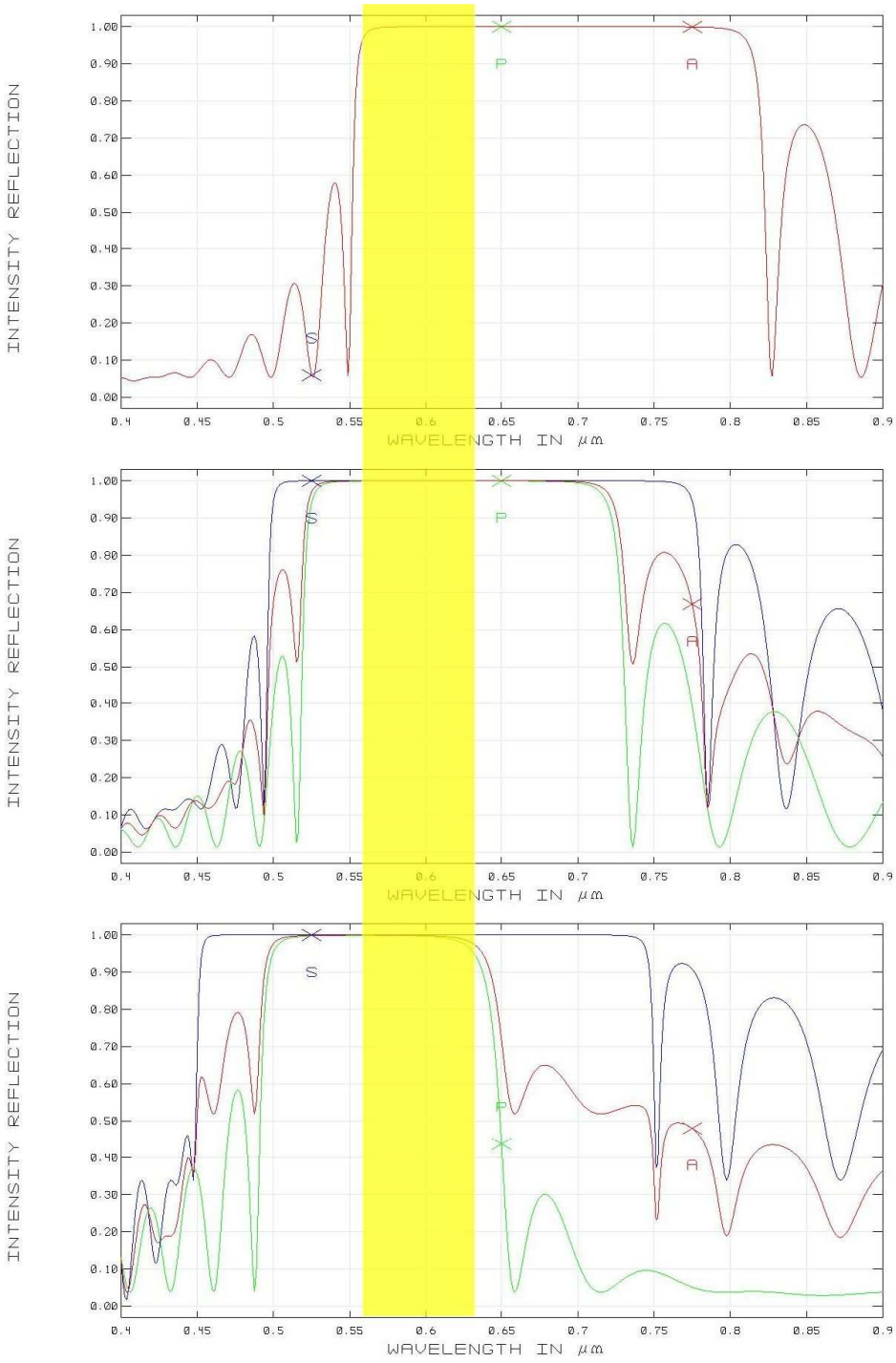

Figure **5-1**: The omnidirectional bandgap of reflector I.

We can see good agreement between the omnidirectional bandgap range and the light intensity of LED. Comparing different reflectors, the reflector II with 560 nm ~ 630 nm omnidirectional bandgap shows the best result. The LED chip is assumed to emit blue light at 440 nm and the phosphor media to emit yellow light at 560 nm. By using reflector I, the yellow light exiting the LED apparently increased compared with no added reflector. However, the blue light also decreased when the reflector was added. As mentioned in Chapter 4, the reflectance spectrum shifts to the shorter wavelength region. Though the reflector shows very high transmittance in the blue light region for the normal incidence, the transmittance may lower while the incidence angle increases. The yellow light also decreases because less blue light strikes the phosphor medium. While the bandgap of reflector I is 550 nm ~ 620 nm and 560 nm ~ 630 nm for reflector II, we expect reflector II to transmit more blue light and excite and reflect more yellow light. This assumption matches our simulation result. For filter III (570 nm ~ 640 nm) and IV (580 nm ~ 650 nm), more blue light passes through the reflector but less yellow light is reflected.

5.2 Increase efficiency by preventing TIR

We change the r/R ratio to see how it will change efficiency, where r is the radius of the inner air hemisphere and R is the radius of exterior encapsulant. Theoretically, if r/R is less than the reciprocal of $n_{encapsulant}$, most of the light will not encounter TIR at the exterior encapsulant/air interface. The smallest r/R to prevent TIR in our experiment is 0.625. The results are shown in Table 5-3.

Table **5-3**: The light intensity for different r/R ratio.

r/R = 0.43	Yellow (W)	Blue (W)	Total (W)
No reflector applied	2.64	3.84	6.48
II (660 nm)	2.78	3.8	6.58
r/R= 0.65	Yellow (W)	Blue (W)	Total (W)
No reflector applied	2.30	3.78	6.08
II (660 nm)	2.34	3.76	6.11
r/R= 0.75	Yellow (W)	Blue (W)	Total (W)
No reflector applied	1.07	3.74	4.81
II (660 nm)	1.15	3.69	4.84

Comparing results by two different r/R values, we can see obvious differences between them. We only change the R value and the light intensity drops while r/R exceeds 0.625. The light trapped in the encapsulant has long path lengths and consequently encounters increased loss. The hemisphere design with proper r/R ratio successfully prevents TIR and increases light extraction efficiency.

Chapter 6

Conclusion

The thesis presents an efficient white light pc-LED scheme. The high efficiency is achieved by reflecting the backward phosphor emission and reducing the loss due to TIR at the exterior interface. In a pc-LED, more than 50% of the yellow light goes backward to the LED chip, placing a reflector between the LED chip and phosphor layer could recycle the backward light to the forward direction. According to the simulation by ZEMAX, the yellow emission from the phosphor medium was enhanced by 5%. In addition, the hemispherical structure with proper r/R ratio could minimize TIR at the exterior interface. The TIR may result in internal loss of light trapped in the encapsulant. For the optimal r/R ratio, the yellow light exiting the encapsulant could be doubled compared to the design which encounters TIR.

References

[1] Fukuda, M., 1999. *Optical Semiconductor Devices*. New York: John Wiley & Sons.

[2] Holonyak, N. Jr. and S. F. Bevaqua, 1962. Coherent (visible) light emission from Ga(As1-xPx) junctions. *Applied Physics Letters* 1:82-83.

[3] Holcomb, M. P. Grillot, G. Hofler, M. Krames and S. Stockman, 2001. AlGalnP LEDs break performance barriers. *Compound Semiconductor* 59:

[4] Johnson, S., 2002. LEDs—An overview of the state of the art in technology and application. *Light Right 5 Conference*, 27-31.

[5] Steigerwald, D. A., J. C. Bhat, D. Collins, R. M. Fletcher, M. Ochiai Holcomb, M. J. Ludowise, P. S. Martin, and S. L. Rudaz, 2002. Illumination with solid state lighting technology. *IEEE Journal of Selected Topics in Quantum Electronics* 8:310-320.

[6] Schnitzer, I., E. Yablonovitch, C. Caneau, and T. J. Gmitter, 1993. Ultrahigh spontaneous emission quantum efficiency, 99.7% internally and 72% externally, from AlGaAs/GaAs/AlGaAs double heterostructures. *Applied Physics Letters* 62:131-133.

[7] Schubert, E.F.,2006. *Light Emitting Diodes, 2nd Edition*, Cambridge University Press, Cambridge , UK..

[8] Yeh, P., 1988. *Optical Waves in Layered Media*. New York: John Wiley & Sons.

[9] Krames, M. R., O. B. Shchekin, R. Mueller-Mach, G. O. Mueller, L. Zhou, G. Harbers, and M. G.Craford, 2007. Status and future of high-power light-emitting diodes for solid-state lighting. *Journal of Display Technology* 3:160-175.

[10] Narendran, N., Y, Gu, J. Freyssinier, and Y. Zhu, 2005. Extracting phosphor-scattered photons to improve white LED efficiency. *Phys. Stat. Sol.* (a) 202(6), R60-R62.

[11] Yamada, K., Y. Imai and K. Ishii, 2003. Optical simulation of light source devices composed of blue LEDs and YAG phosphor. *Journal of Light and Visual Environment* 27(2):70-74.

[12] Chen, H., 1997. LED structure with ultraviolet-light emission chip and multilayered resins to generate various colored lights.. US Patent 5,962,971, filed Aug. 29, 1997, and issued Oct. 5, 1999.

[13] Lowery, C. H., 1998. Multiple encapsulation of phosphor-LED devices. US Patent 5,959,316, filed Sept. 1, 1998, and issued Sept. 28, 1999.

[14] Duggal, A., A. M. Srivastrava, J. M. Davenport, T. F. Soules, and W. W. Beers, 2001. Phosphors for white light generation from UV emitting diodes. US Patent 6,294,800 B1, filed Nov. 30, 1998, and issued Sept. 25, 2001.

[15] Zhu, Y. and N. Narendran, 2008. Optimizing the Performance of Remote Phosphor LEDs. *Journal of Light and Visual Environment* 32(2):115-119.

[16] Luo, H, 2005. Analysis of high-power packages for phosphor-based white-light-emitting diodes, *Applied Physics Letters* 86.

[17] Liu, Z., S. Liu, K. Wang, and X. Luo, 2008. ”Effects of phosphor’s location on LED packaging performance”. Electronic Packaging Technology & High Density Packaging, 2008. ICEPT-HDP 2008. International Conference on , vol., no., pp.1-7, 28-31 July 2008

[18] Oh, J. R. , S. H. Cho, Y. H. Lee, and Y. R. Do, 2009. Enhanced forward efficiency of $Y_3Al_5O_{12}:Ce^{3+}$ phosphor from white light-emitting diodes using blue-pass yellow-reflection filter. *Optics Express* 17:7450-7457.

[19] Kochergin, V., 2003. *Omnidirectional Optical Filters*. Boston: Kluwer Academic Publishers.

[20] Deopura, M., C. K. Ullal, B. Temelkuran, and Y. Fink, 2001. Dielectric omnidirectional visible reflector. *Optics Letters* 26:1197-1199.

[21] Allen, S. C. and A. J. Steckl, 2008. A nearly ideal phosphor-converted white light-emitting diode. *Applied Physics Letters* 92.

[22] E. Fred Schubert. "Inorganic Semiconductors for Light-emitting Diodes", Organic Light Emitting Devices,